Progress In Electromagnetics Research C, Vol. 82, 89–97, 2018

Folded-Slot Active Tag Antenna for 5.8 GHz RFID Applications

Sudhir Bhaskar*, Sarthak Singhal, and Amit K. Singh

Abstract—In this paper, a folded slot active tag antenna for 5.8 GHz radio frequency identification (RFID) applications is presented. It consists of an inverted U-shaped monopole radiator fed by a coplanar waveguide (CPW) feed line and extended ground planes. A 10 dB return loss bandwidth of 5.65–6.55 GHz is achieved. The overall volume of the presented antenna is $10.7 \times 11 \times 1.6\,\text{mm}^3$. A good agreement between the simulated and measured results is observed. The antenna has an omnidirectional radiation pattern at 5.8 GHz which makes it suitable for RFID applications. It has advantages of compact dimensions and wider bandwidth than previously reported structures.

1. INTRODUCTION

Radio frequency identification (RFID) is a technology for the contactless automatic identification. By using this technology, items can be identified and tracked. An RFID system consists mainly of three system components: tag or transponder, reader, and data processing system. An RFID tag contains two main parts, viz. application specific integrated circuit (ASIC) and an antenna. It has to be attached to the object of interest. An RFID reader or transceiver is used to read and write data from the tag remotely. The data processing system comprises a host computer and software to analyze the received data. During the last decade, researchers have shown a lot of interest in RFID due to its extensive applications in electronic transport payment, access control, automotive security, automated libraries, healthcare industries, livestock management, etc. [1]. There are four different frequency bands allocated for RFID applications. They are low frequency (LF, 125–134 kHz), high frequency (HF, 13.56 MHz), ultra-high frequency (UHF, 860–960 MHz) and microwave frequency (2.4 GHz, 5.8 GHz and 24 GHz). Different countries have allocated different frequency bands for UHF-RFID applications; e.g., China (840–845 MHz), Europe (866–869 MHz), USA (902–928 MHz) and Australia (920–926 MHz). At LF and HF bands, the dimensions of the tag antenna are larger since the wavelength is larger, resulting in a small read range between the tag and the reader. Due to above discussed problems related to the frequency bands other than the microwave band, the operability of unlicensed microwave frequency band RFID tags has attracted researchers from all over the world. In order to achieve a larger read range with a miniaturized size, the microwave frequency band is more suitable, as it can be used for automatic toll collection, traffic control and biomedical applications.

For a miniature RFID tag, the tag antenna should be platform tolerant with compact dimensions and an omnidirectional radiation pattern [2, 3]. RFID tags can be divided into two categories: one is a passive tag, and the other is an active tag. Passive tags do not require an internal power source. They are energized by the reader signal. In a passive RFID tag, input impedance of the antenna is matched with the conjugate impedance of the tag IC for maximum power transfer from antenna to chip [4]. Passive RFID microchips have capacitive impedances. Thus, the antenna is designed with a larger inductive input impedance. Active RFID tags are powered up by internal batteries. An active RFID tag IC has a 50 Ω input impedance for which the active RFID tag antenna needs to be matched

Received 9 January 2018, Accepted 6 March 2018, Scheduled 20 March 2018
* Corresponding author: Sudhir Bhaskar (sbhaskar.rs.ece@iitbhu.ac.in).
The authors are with the Department of Electronics Engineering, Indian Institute of Technology (BHU), Varanasi, India.

with a 50 Ω microchip. In the available literature, several passive RFID tag antenna structures [5–12] and active RFID tag antenna structures [13–21] have already been proposed. They include a meander line antenna [5], in which nonuniform meandering is used for antenna size miniaturization and gain optimized by means of a genetic algorithm. A planar inverted F antenna is presented in [6], which has a platform independent impedance behavior. A dual-band (900 MHz and 2.45 GHz) antenna for passive RFID tag applications with a coupled slot feed structure is proposed in [7]. In this design, the impedance of the tag microchip is assumed as 50 Ω. In [8], a single-sided dual-band antenna for UHF (915 MHz) and SHF (2450 MHz) frequencies is explored. That structure has a dual antenna characteristic for the 915 MHz band and a single antenna characteristic for the 2450 MHz frequency band. The dual antenna at UHF band is used for a higher read range. Single feed circular polarized antennas have been reported in [9, 10] for minimization of polarization mismatching between reader and tag antennas. In [9], a circularly polarized loop antenna is proposed for the UHF band with an input impedance of $13.5 + j111\,\Omega$ whereas in [10] a square microstrip antenna is proposed for the 2.45 GHz band with an input impedance of 50 Ω. In [11, 12], antennas with a first-order Hilbert fractal design are proposed for microwave/UHF band RFID applications. An inverted-F antenna for X-band active RFID applications has been devised in [10]. A balanced feed asymmetric dipole antenna in [14] has been designed for 2.45 GHz active RFID tags, and dual environment active tag antennas are proposed in [15–17]. In free space these dual antennas work as dipole antennas, and the metallic surface works as a patch. Folded-slot CPW-fed monopole antennas for 5.8 GHz applications are presented in [18–24]. In these antennas different folded slot patterns are inserted onto a single-sided substrate with the slot length nearly equal to the guided wavelength at resonance. These previously reported structures have large dimensions in comparison to the reduced dimensions of devices into which these RFID tags are supposed to be attached.

This article is a comprehensive report of [25] with a detailed parametric study and more experimental results. In this paper, a planar monopole antenna comosed of an inverted U-shaped radiating patch with a folded slot and a CPW feed structure is presented. Coplanar waveguide (CPW) feeding technique is used due to a number of advantages such as easy fabrication, low radiation losses and the requirement of only a single layer substrate. The resonance at 5.8 GHz frequency is achieved by loading a folded slot on a rectangular patch. The overall dimensions of the antenna are reduced due to the folded slot technique, and resonating frequency of the antenna can be adjusted by fine tuning of the slot length. The proposed antenna has advantages such as compact size, large impedance bandwidth, and good radiation characteristics.

2. ANTENNA CONFIGURATION

The optimized geometry of the proposed antenna is shown in Fig. 1, and its optimized dimensions are listed in Table 1. An FR-4 glass epoxy substrate, with thickness $h = 1.6$ mm, dielectric constant $\varepsilon_r = 4.4$ and loss tangent $\tan\delta = 0.02$, is used to design the proposed antenna. An inverted U-shaped folded slot is cut down on a rectangular patch of dimensions $10.7 \times 11\,\text{mm}^2$. That folded slot isolates the radiating inverted U-shaped patch from the CPW ground plane. The geometrical dimensions of the proposed antenna are optimized with the help of Finite Element Method (FEM) based Ansoft's HFSS simulation software [26]. The antenna is symmetrical with respect to Y-axis.

From the basic antenna design theory, the length of the radiating element should be proportionate to the wavelength of the operating frequency. So for an antenna resonating at 5.8 GHz, the antenna length

Table 1. Optimized parameters of the antenna.

Parameter	Dimensions	Parameter	Dimensions
L_{sub}	10.7 mm	S_w	0.8 mm
W_{sub}	11 mm	L_{s1}	8.5 mm
L_f	7.0 mm	L_{s2}	3.0 mm
W_f	1.0 mm	h	1.6 mm

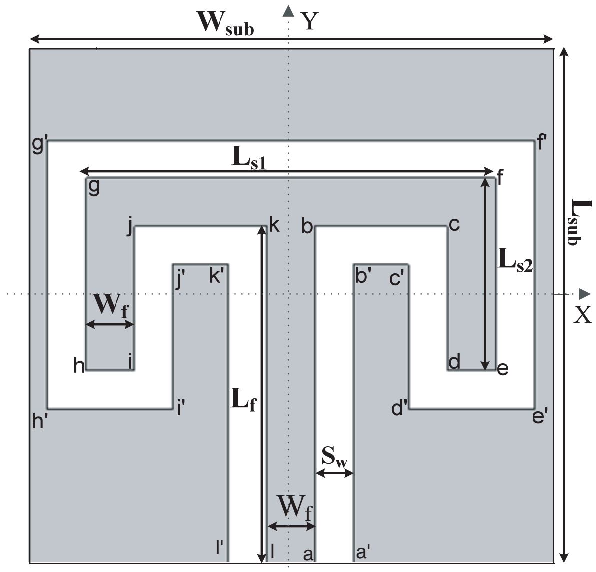

Figure 1. Configuration of the antenna.

should be approximately 52 mm. The total inner length of the folded slot is 44 mm ($abcdefghijkl$), and total outer length of the folded slot is 47.20 mm ($a'b'c'd'e'f'g'h'i'j'k'l'$) or about 0.85–0.91 of wavelength relative to the resonant frequency at 5.8 GHz as follows:

$$\text{path abcdefghijkl} = 2\,(L_f + L_{s1} + 2L_{s2}) - 3W_f \quad (1)$$

$$\text{path } a'b'c'd'e'f'g'h'i'j'k'l' = \text{path } abcdefghijkl + 4S_w \quad (2)$$

This demonstrates that the antenna gets miniaturized by means of the folded slot technique.

3. PARAMETRIC ANALYSIS

Since every geometrical parameter affects the antenna performance, parametric analysis is carried out by varying one parameter at a time and keeping other parameters constant. During parametric analysis, a few parameters like slot width (S_w), conducting strip width (W_f), L_{s1} and L_{s2} of antenna are varied. The effects of these parameters on antenna performance are discussed as follows.

3.1. Effects of Slot Width ($\mathbf{S_w}$)

In order to examine the effect of slot width on the antenna performance, the slot width is varied from 0.7 mm to 0.9 mm. The reflection coefficient versus frequency characteristics for these slot width values are presented in Fig. 2. It is observed that the resonance frequency decreases with increase in the slot width. This phenomenon occurs due to the increase in the outer length of the folded slot according to Equation (2). The total increase in the outer slot length is four times of the increase in S_w and vice versa. The slot width does not affect the inner length of the folded slot. At the optimized slot width of 0.8 mm, the resonance is at 5.8 GHz.

3.2. Effects of Conducting Strip Width ($\mathbf{W_f}$)

After examining the effect of slot width (S_w), the effect of conducting strip width (W_f) is studied by varying it from 0.8 mm to 1.2 mm. Fig. 3 demonstrates that the resonance frequency shifts to a higher frequency with increase in W_f. This is because the increase in W_f reduces the inner and outer lengths of the folded slot in both equations. The desired resonance is observed at the strip width of 1 mm.

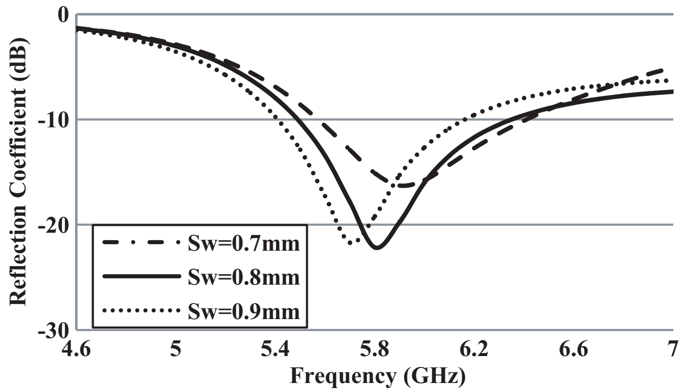

Figure 2. Reflection coefficient characteristics for different slot widths S_w.

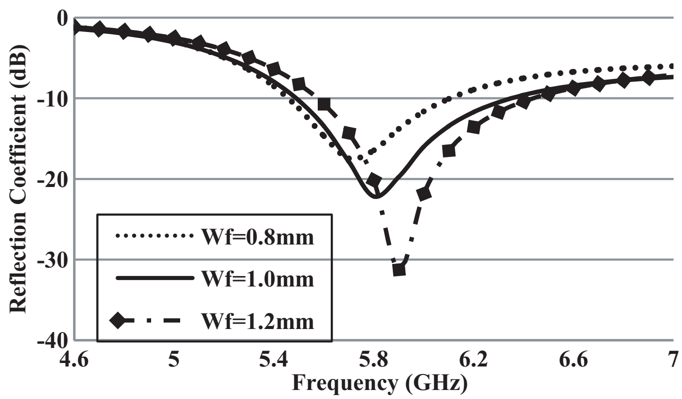

Figure 3. Frequency response of reflection coefficient with various conducting strip widths W_f.

3.3. Effects of Different Values of Length L_{s2}

According to Equations (1)–(2), the change in total slot length is quadruple of the change in L_{s2}. So, the resonance frequency must shift towards the lower frequency with increase in L_{s2}. The same phenomenon is illustrated by Fig. 4 for a variation from 2 mm to 4 mm. It is observed that the desired resonance is achieved for $L_{s2} = 3$ mm.

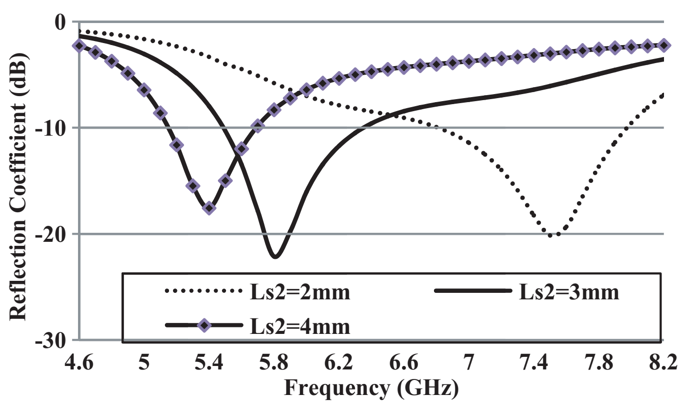

Figure 4. Reflection coefficient characteristics for different values of parameter L_{s2}.

3.4. Effects of Different Values of Length L_{s1}

In order to analyze the effect of variation of parameter L_{s1} on resonating frequency, the antenna is simulated with different L_{s1} values while keeping other parameters (S_w, W_f, L_{s2}) constant. For the desired resonating frequency antenna is optimized at $L_{s1} = 8.5$ mm. In Fig. 5, reflection coefficient of antenna is depicted as a function of frequency with variable parameter L_{s1}.

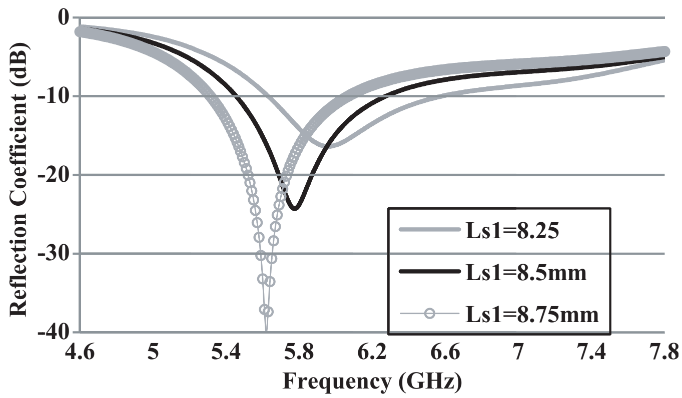

Figure 5. Reflection coefficient versus frequency characteristics for variation in parameter L_{s1}.

4. RESULTS AND DISCUSSION

The fabricated prototype of the proposed antenna structure is shown in Fig. 6. Anritsu's MS2038C VNA is used for the measurement of the fabricated antenna. Fig. 7 shows the measured and simulated reflection coefficient characteristics of the designed antenna. It is observed that the measured and simulated results are in good agreement. The simulated impedance bandwidth is 14.52% (860 MHz) whereas the experimental impedance bandwidth is 15.25% (900 MHz). The simulated resonance is at 5.8 GHz and measured resonance at 5.9 GHz. The discrepancies between the simulated and experimental results are due to fabrication errors, soldering imperfections and manual errors while performing the experimental measurements.

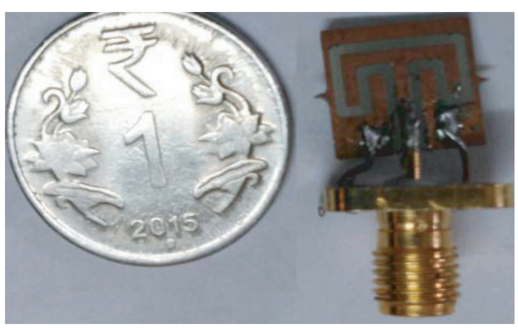

Figure 6. Fabricated antenna prototype.

The simulated and experimental input impedances of the proposed antenna are shown in Fig. 8. At the resonant frequency of 5.8 GHz, the imaginary part is close to zero, and real part is approximately equal to 50 ohm. These values of real and imaginary parts indicate that the input impedance is approximately 50 Ω at the desired resonance. This leads to the observation that a good impedance matching is achieved between the antenna and the coaxial probe, which reduces the losses occurring due to reflections.

A comparison of the designed antenna with previously reported structures in terms of dimensions and bandwidth is given in Table 2. All the compared folded slot antennas are designed with a 1.6 mm

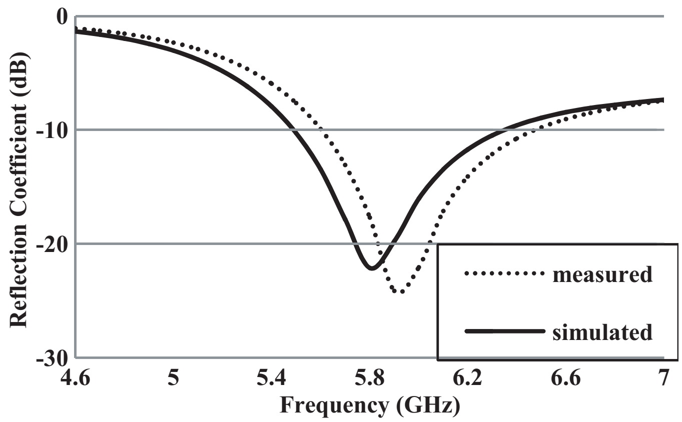

Figure 7. Simulated and measured reflection coefficient verses frequency characteristics.

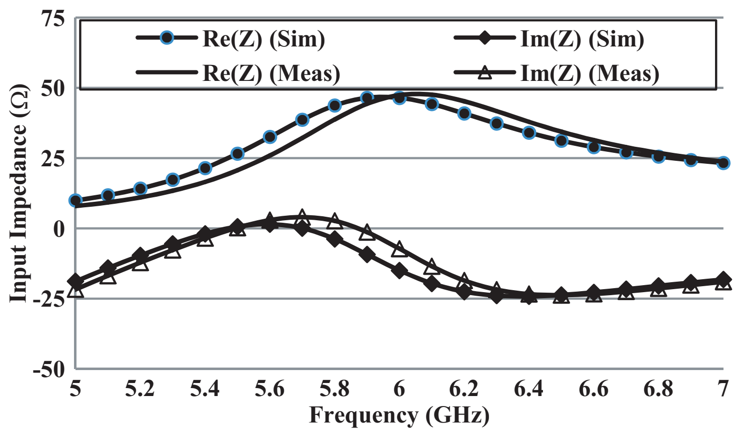

Figure 8. Input impedance of proposed antenna.

thick FR4 substrate and operate at 5.8 GHz resonant frequency. It is observed that the designed antenna has the smallest dimensions except one antenna [22]. However, that folded strip antenna has a narrow bandwidth around 5.8 GHz. The ratio of percentage bandwidth and the antenna size of the proposed antenna is the largest next only to the antenna in [18]. Although the antenna of [18] has bandwidth two times wider than the proposed antenna, the proposed antenna is 17.69 percent smaller in size.

Table 2. Comparison of proposed antenna and reported antennas.

Published Literature	Antenna size in mm^3	Operating band (GHz)	% Bandwidth	% size reduction
[18]	$13 \times 11 \times 1.6$ (228.8)	5.09–6.83	30	17.69
[19]	$16.8 \times 13 \times 1.6$ (349.44)	5.52–6.16	11	46.10
[20]	$15 \times 10 \times 1.6$ (240)	5.63–6.12	8	21.53
[21]	$30 \times 30 \times 1.5$ (1350)	5.67–6.11	7.5	86.05
[22]	$14 \times 8 \times 1.6$ (179.2)	5.53–5.98	6.2	−5.08
[23]	$16 \times 15 \times 1.6$ (384)	5.4–6.9	26	50.95
Proposed antenna	$11 \times 10.7 \times 1.6$ (188.32)	5.65–6.55	15.25	-

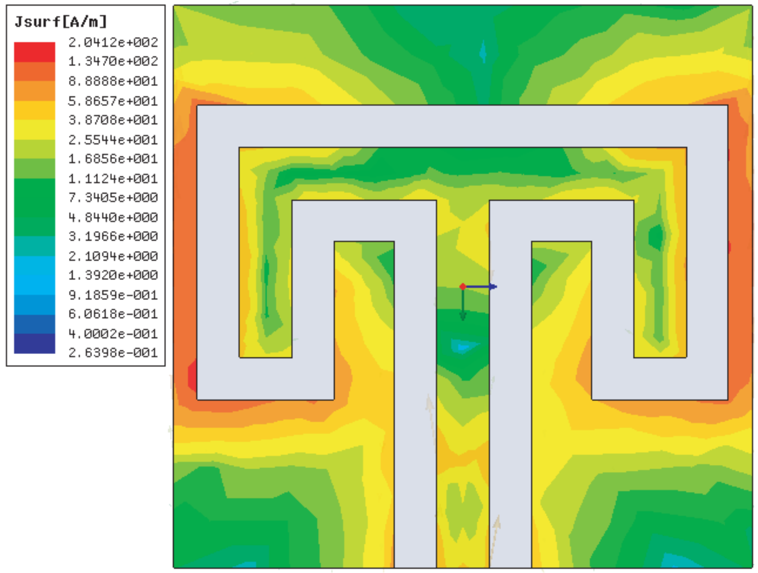

Figure 9. Surface current distribution at operating frequency 5.8 GHz.

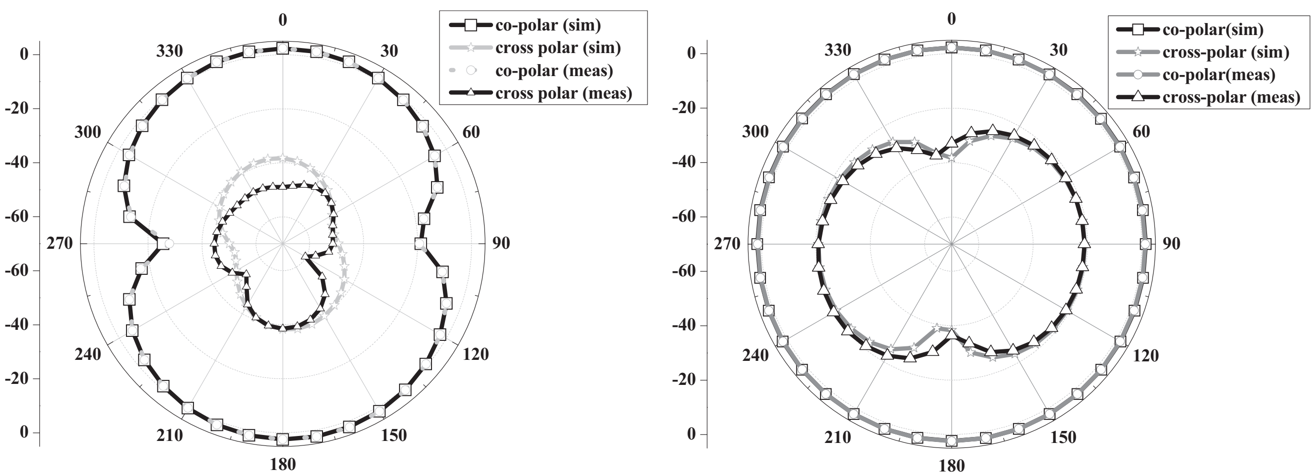

Figure 10. Co-polar and cross-polar radiation patterns at 5.8 GHz. (a) E-plane pattern. (b) H-plane pattern.

Figure 9 shows the surface current density distribution at operating frequency 5.8 GHz. It is detected that the magnitude of surface current density around the folded slot is comparatively high which implies that maximum of surface current is concentrated around the slot. This surface current density plot signifies that operating frequency of the antenna can be adjusted by varying the length of the folded slot.

The measured and simulated predominant E-plane and H-plane radiation patterns of the proposed antenna at the operating frequency 5.8 GHz are exhibited in Figs. 10(a)–(b). Both co-polar and cross-polar radiation patterns are measured. The co-polar patterns have bi-directional nature in the E-plane (x-y plane) and are omnidirectional in the H-plane (x-z plane). It is observed that in the E-plane, the maximum level of the co-polar pattern is 40.46 dB more than that of the cross-polar pattern. In H-plane patterns, this difference between the two levels is 23.04 dB.

Figure 11 shows the measured and simulated antenna gains for the designed antenna. At the resonance of 5.8 GHz, the simulated maximum gain is 2.47 dB, and measured peak gain is 2.38 dB.

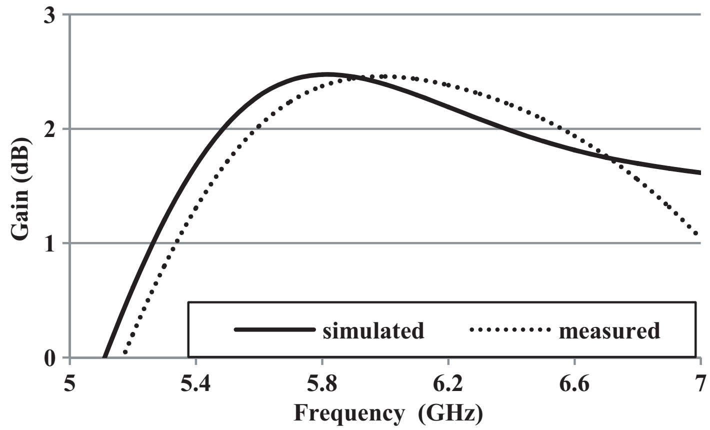

Figure 11. Antenna gain for proposed antenna.

5. CONCLUSION

In this paper, a miniature coplanar waveguide fed folded slot monopole antenna is studied and implemented for 5.8 GHz active RFID tag applications. The designed tag antenna comprises 900 MHz bandwidth. A maximum gain of 2.4 dB is achieved. The designed antenna has overall volume of $10.7 \times 11 \times 1.6\,\text{mm}^3$, which is smaller than those of previously reported structures. The omnidirectional radiation characteristic and miniaturized size of designed antenna make it suitable not only for RFID applications but also for wireless applications at 5.8 GHz.

REFERENCES

1. Chawla, V. and D. S. Ha, "An overview of passive RFID," *IEEE Communication Magazine*, Vol. 45, 11–17, September 2007.
2. Hirvonen, M., K. Jaakkola, P. Pursula, and J. Saily, "Dual-band platform tolerant antennas for radio-frequency identification," *IEEE Transactions on Antennas and Propagation*, Vol. 54, No. 9, 2632–2637, September 2006.
3. Hamani, A., M. C. E. Yagoub, T. P. Vuong, and R. Touhami, "A novel broadband antenna design for UHF RFID tags on metallic surface environments," *IEEE Antennas and Wireless Propagation Letters*, Vol. 16, 91–94, 2017.
4. Marrocco, G., "The art of UHF RFID antenna design: Impedance-matching and size-reduction techniques," *IEEE Antennas Propag. Mag.*, Vol. 50, 66–79, 2008.
5. Marrocco, G., "Gain-optimized self-resonant meander line antennas for RFID applications," *IEEE Antennas and Wireless Propagation Letters*, Vol. 2, 302–305, 2003.
6. Hirvonenen, M., P. Pursula, K. Jaakkola, and K. Laukkanen, "Planar inverted-F antenna for radio frequency identification," *Electronics Letter*, Vol. 40, No. 14, 848–850, July 2004.
7. Jeon, S., Y. Yu, and J. Choi, "Dual-band slot-coupled dipole antenna for 900 MHz and 2.45 GHz RFID tag application," *Electronics Letters*, Vol. 42, No. 22, October 2006.
8. Kamalvand, P., G. K. Pandey, and M. K. Meshram, "RFID tag antenna for ultra and super high frequency band applications," *International Journal of RF and Microwave Computer-aided Engineering*, Vol. 26, No. 7, 640–650, September 2016.
9. Chen, H. D., C. H. Tsai, C. Y. D. Sim, and C. Y. Kuo, "Circular polarized loop tag antenna for long reading range RFID applications," *IEEE Antennas and Wireless Propagation Letter*, Vol. 12, 1460–1463, November 2013.
10. Nguyen, D. L., K. S. Paulson, and N. G. Riley, "Reduced size circular polarized square microstrip antenna for 2.45 GHz RFID applications," *IET Microw. Antennas Propag.*, Vol. 6, No. 1, 94–99, 2012.

11. Shi, Y., K. Qi, and C. H. Liang, "A miniaturized design of 2.45 GHz RFID tag antenna," *Microwave and Optical Technology Letters*, Vol. 57, 1905–1908, 2015.
12. Shi, Y., C. Fang, K. Qi, and C. H. Liang, "A broadband design of UHF fractal RFID tag antenna," *Progress In Electromagnetics Research Letters*, Vol. 58, 45–51, 2016.
13. Pazin, L., A. Dyskin, and Y. Leviatan, "Quasi-isotropic X-band inverted-F antenna for active RFID tags," *IEEE Antennas and Wireless Propagation Letter*, Vol. 8, 27–29, April 2009.
14. Fang, Z., R. Jin, and J. Geng, "Asymmetric dipole antenna suitable for active RFID tags," *Electronics Letters*, Vol. 44, No. 2, 937–939, January 2008.
15. Malek, M. A., S. Hakimi, S. K. A. Rahim, and A. K. Evizal, "Dual-band CPW-fed transparent antenna for active RFID tags," *IEEE Antennas and Wireless Propagation Letter*, Vol. 14, 919–922, April 2015.
16. Chang, L., H. Wang, Z. Zhang, Y. Li, and Z. Feng, "Compact single-feed dual-mode antenna for active RFID tag applications," *IEEE Transaction on Antennas and Propagation*, Vol. 63, No. 11, 5190–5194, November 2015.
17. Chang, L., H. Wang, Z. Zhang, Y. Li, and Z. Feng, "A dual-environment active RFID tag antenna mountable on metallic objects," *IEEE Antennas and Wireless Propagation Letter*, Vol. 15, 1759–1762, November 2016.
18. Liu, W. C. and Z. K. Hu, "Broadband CPW-fed folded-slot monopole antenna for 5.8 GHz RFID application," *Electronics Letters*, Vol. 41, No. 7, 937–939, August 2005.
19. Liu, W. C. and C. M. Wu, "CPW-fed shorted F-shaped monopole antenna for 5.8-GHz RFID applications," *Microwave and Optical Technology Letters*, Vol. 48, No. 3, 573–575, March 2006.
20. Liu, W. C., "A coplanar waveguide-fed folded-slot monopole antenna for 5.8 GHz radio frequency identification application," *Microwave and Optical Technology Letters*, Vol. 49, No. 1, 71–74, January 2007.
21. Chen, S. Y. and P. Hsu, "CPW-fed folded-slot antenna for 5.8 GHz RFID tags," *Electronics Letters*, Vol. 40, 1516–1517, November 2004.
22. Liu, W. C. and P. C. Kao, "Compact CPW-fed dual folded-strip monopole antenna for 5.8-GHz RFID application," *Microwave and Optical Technology Letters*, Vol. 48, No. 8, 1614–1615, August 2006.
23. Ma, D. and W. X. Zhang, "Broadband CPW-fed RFID antenna at 5.8 GHz," *Electronics Letters*, Vol. 42, No. 22, 1516–1517, October 2006.
24. Zhang, M. T., Y. C. Jiao, and F. S. Zhang, "Dual-band CPW-fed folded-slot monopole antenna for RFID application," *Electronics Letters*, Vol. 42, No. 21, October 2006.
25. Bhaskar, S., S. Singhal, and A. K. Singh, "CPW-fed inverted U-shaped folded-slot monopole antenna for RFID applications," *National Conference on Recent Advancement in Communication Engineering and Microelectronics (RACEM)*, MMMUT Gorakhpur, India, March 9–10, 2016.
26. Ansoft Corporation, HFSS, High frequency structure simulator version 11, Finite element package, Ansoft Corporation, Available at: http://www.ansoft.com.